United States Department of the Interior

Geological Survey

VOLCANIC GLASS COMPOSITIONS FROM TWO SPREADING CENTERS IN LAU BASIN, SOUTH PACIFIC OCEAN

by

Alicé S. Davis, David A. Clague, and Janet L. Morton

Open File Report 87-61

Menlo Park, California

1986

INTRODUCTION

Volcanic rocks ranging from basalt to andesite in composition were dredged from Lau Basin. Samples labeled L3-84-SP were dredged during a U.S. Geological Survey cruise of the R/V S.P. Lee from two sites on Valu Fa Ridge, a spreading center in the southern Lau Basin. Samples designated SO35-2 were dredged during a Bundesanstalt fur Geowissenschaften und Rohstoffe cruise of the F/S Sonne from 24 sites in Lau Basin. Fifteen of these dredges were also located on, or near, Valu Fa Ridge, and ten dredges were located on a spreading center north of Valu Fa Ridge. Location of the two areas studied are shown in Figure 1 and bathymetry and dredge locations in the northern and southern study area are shown in Figures 2 and 3, respectively. Dredge locations and water depths are listed in Table 1. The rocks recovered from the northern study area are primarily pillow basalt or pahoehoe flow fragments with fresh glass rinds. In the southern study area roughly-shaped aa-like flows predominate and pillows are uncommon. However, fresh glass is also abundant on the aa flow fragments.

This paper reports major and minor element compositions of 44 volcanic glasses and compares them with the fractionated mid-ocean ridge suite of glasses from the Galapagos rift zone and with glasses from the Troodos ophiolite.

GEOLOGIC SETTING

Lau Basin is an actively spreading back-arc basin located behind the Tonga island arc. It is an elongate, south-verging interarc basin between the Tonga-Kermadec Ridge, forming the frontal arc, and the Lau-Colville Ridge which forms a remnant arc (Karig, 1971). The axis of spreading consists of a complex series of north-northeast trending ridges. The spreading center in the southern part of Lau Basin, Valu Fa Ridge, is located near the eastern side of the basin. Valu Fa Ridge is a narrow ridge that rises to a minimum water depth of 1600 m. Valu Fa Ridge extends from at least latitude 20°40' S to 22°40' S and is offset 3 km left-laterally at latitude 22°12' S. Magnetic anomaly patterns indicate that the rate of spreading is about 7 cm/yr and that the present ridge has been actively spreading for at least 0.7 to 0.9 million years (Morton and Sleep, 1985). A flat-topped magma chamber, identified by seismic refraction and reflection lines at latitudes 22°18'S and 22°27'S (Morton and Sleep, 1985), lies about 3.5 km beneath the ridge. The magma chamber appears to be continuous along the strike of the ridge becoming narrower northward, (2 km at 22°18'S and 3km at 22°27'S), and probably terminates at latitude 22°12'S where the ridge is offset to the west.

Farther north, near latitude 18°40'S, the basin is wider (Hawkins and Melchior, 1985) and the spreading center is located approximately eqidistant from the margins of the basin. Here, the spreading ridge is somewhat deeper, rising to a minimum water depth of 2200 m (von Stackelberg, et al., 1985).

METHODS

Fragments of glass were chosen from selected samples of each dredge for major and minor element analyses by electron microprobe. The glass fragments were washed in distilled water and then were mounted in epoxy resin and polished. All glass samples were analyzed with an accelerating voltage of 15 kv and sample current of 10 nAmps for maximum count times of 40 seconds.

Glasses with minor amounts of microlites were analyzed with a stationary beam (~50 μ). Glasses with abundant microlites were analyzed using a raster beam scanning an area of approximately 100 by 100 μ. Natural basalt glasses VG-2 and A-99 and andesitic glass GSC were used as standards. Standards were run at the beginning and interspersed throughout the analyses. Precision and accuracy of major elements are better than ± 2%, and are usually good to ± 1% for all major elements except Na and Si. For K, P, and S accuracy and precision are probably not better than ± 5%. All microprobe data were reduced using a modified version of the Bence-Albee method (Bence and Albee, 1968).

GLASS COMPOSITIONS

Major and minor element contents of volcanic glasses recovered on cruise L3-84-SP are presented in Table 2, and those recovered on cruise SO35-2 are presented in Tables 3 and 4. Selected oxides have been plotted on MgO variation diagrams and are shown in Figures 4 to 8. Glasses from the two geographic areas are distinct. Compositions from the northern area resemble low-K_2O mid-ocean ridge basalt (N-MORB), whereas compositions from the southern area are predominantly andesite and minor basaltic andesite and one sample of island arc basaltic andesite.

Northern Study Area

Nine samples (SO35-2 2KD to 62KD) from the northern area resemble N-MORB but range from relatively primitive (25KD--MgO=9.14%) to evolved ferrobasalt (49KD--MgO=6.03, FeO=13.8%). All of the samples are olivine-normative, with olivine ranging from 2.3 to 17.8%. Major oxides have well developed linear trends of CaO (Fig. 5a) and Al_2O_3 (Fig. 4b) decreasing with decreasing MgO, whereas SiO_2, Na_2O, K_2O, P_2O_5, FeO^T, and TiO_2 increase with decreasing MgO (Figs. 4a, 5b, 6, 7,respectively). Such trends, commonly observed in mid-ocean ridge basalt, reflect olivine+plagioclase±clinopyroxene fractionation. P_2O_5 shows a narrow linear correlation with K_2O (Fig. 9) suggesting that the mantle source for these lava samples is homogeneous in K_2O/P_2O_5.

Totals greater than 99% for most samples indicate that volatile elements are present only in minor amounts, as is typical in MORB. Sulfur ranges from 880 ppm in the least fractionated sample (25KD) to 1260 ppm in the most fractionated ferrobasalt (49KD) and has a well defined positive correlation with FeO (Fig. 8b) resulting from the increased solubility of sulfur in a melt with increasing FeO (Mathez, 1976). Juvenile sulfur contents of MORB have been estimated to be between 800 and 900 ppm (Moore and Fabbi, 1971). All of the MORB-like samples were dredged from water depths greater than 2000 m and were quenched under hydrostatic pressure great enough to inhibit degassing.

Similar MORB-like compositions have previously been reported from Lau Basin by Hawkins (1976) and Hawkins and Melchior (1985), who reported a greater compositional range with N-MORB compositions restricted to the central part of the northern basin and more arc-like compositions from the margins. The samples analyzed here are all from the central part of the northern basin and in agreement with the distribution of lava compositions proposed by Hawkins and Melchior (1985).

Southern Study Area

Thirty-two of the thirty-five samples from the southern study area are low-K_2O andesite; two are basaltic andesite (84KD, 68 KD), and one, dredged from a location slightly east of Valu Fa Ridge, resembles an island arc basaltic andesite (87KD). All of the samples are quartz-normative with quartz ranging from 4.5 to 18.9%. The microprobe analyses have low totals, typically around 97.5%. The glasses show no evidence of alteration, hence, low totals suggest large amounts of volatiles, as do the abundant vesicles (30-50%). MgO variation diagrams (Figs. 4-8) show compositional trends that differ significantly from that of samples from the northern area. SiO_2, Na_2O, K_2O, P_2O_5, and TiO_2 show a general increase with decreasing MgO, similar to that of samples from the northern area. However, they do not form an extension of the same trend, and show much more scatter. CaO (Fig. 5a) decreases with decreasing MgO but Al_2O_3 (Fig. 4b) shows no trend. FeO^T (Fig. 7a) shows a generalized trend of increasing with decreasing MgO to about 4% MgO and then decreases reflecting fractionation of an iron-bearing phase such as titanomagnetite. However, considerable scatter in the FeO contents and lack of a matching trend in TiO_2 (Fig. 7b) suggest multiple differentiation trends involving titanomagnetite ±clinopyroxene. Plots of K_2O vs. P_2O_5 (Fig. 9a) and TiO_2 vs. K_2O (Fig. 9b) suggest multiple sources, distinct from that of the northern area, may have been involved. The K_2O/P_2O_5 ratio (Fig. 9a) of the island arc basaltic andesite (~8) differs significantly from both the andesitic (~2) and the MORB-like suite (~1).

Compared with samples from the northern area all samples are low in S (30-378 ppm). Sulfur content of andesitic magma is typically lower than that of associated basaltic magma because S solubility decreases with increased oxygen fugacity and decreased temperatures (Gill, 1981). All of the Valu Fa Ridge samples were dredged from water depths greater than 1600 m, yet are vesiculated and appear degassed. Unlike samples from the northern area, S content of Valu Fa Ridge glasses shows no well defined positive correlation with FeO but instead shows considerable scatter (Fig. 8b).

There appears to be a compositional trend along the strike of Valu Fa Ridge (Fig. 10). The least fractionated glass compositions occur at the northern end (84KD and 68KD), becoming more fractionated southward with the most evolved composition (81KD) at about latitude 22°14' S. Still farther south compositions again become less fractionated (91KD, 94KD, and 97KD). At about latitude 22°14' S spatially closely associated lava samples (e.g. 81KD and 127KD) have a compositional range in SiO_2 of 4%. A variation in SiO_2 content of about 2% is also observed for glass chips recovered from the same dredge haul (D1 and D2, Table 2), and suggests that the magma chamber (or chambers) may be compositionally zoned.

Geochemistry of andesite from Valu Fa Ridge, including trace element and Sr, Nd, and Pb isotopic data, has been reported by Jenner et al. (1985) and Vallier et al. (in press).

COMPARISON WITH A FRACTIONATED MID-OCEAN RIDGE SUITE

Glass compositions of samples from the northern area are very similar to N-MORB from the Ecuador and Galapagos rift areas (Byerly, 1980; Fornari et al., 1983). However, fractionated glasses from the southern area are distinct from andesitic glasses of the Galapagos rift zone (Figs. 4-8). SiO_2, K_2O, and CaO contents are similar but FeO^T, TiO_2, and P_2O_5 are significantly higher in Galapagos rift andesites, whereas Al_2O_3 is higher in Valu Fa Ridge samples. Some oxides would appear more similar if normalized values for Valu Fa Ridge samples were used. However, the large volatile content of these andesites is a distinctive characteristic that comparably evolved Galapagos glasses lack. Compositional trends of Galapagos andesite form a direct linear extension with those

of MORB's indicating that the andesites formed by extensive differentiation of the MORB. Compositional trends of Valu Fa ridge andesite indicate that these andesites are not generated by differentiation of a MORB-like parental magma like those from the northern area, nor are they generated by differentiation from an island arc magma. A parental magma intermediate in composition between MORB and an island arc basalt appears best suited, but such composition is not represented in the recovered samples.

COMPARISON WITH GLASSES FROM THE TROODOS OPHIOLITE

Glass compositions of andesites from the southern area show greater similarity with glasses from the Troodos ophiolite than with andesite from mid-ocean ridge spreading centers. At the Troodos ophiolite two distinctive magma suites are present (Robinson et al., 1983). The stratigraphically lower suite is volatile-rich andesite, minor dacite and rare rhyolite. The andesitic suite grades into an overlying basaltic suite, high in Mg, that has been described as having boninitic affinity (Robinson et al., 1983). The evolved andesite suite shows considerable overlap with andesite compositions from Valu Fa ridge (Figs. 4-8) but also includes more typical island arc andesite with lower TiO_2 content. The unfractionated basaltic suite from Troodos ophiolite shows no resemblance to the MORB-like basalt from the northern area, but has strong island arc characteristics with higher SiO_2 and Al_2O_3, and very low TiO_2 contents. The three least fractionated samples from Valu Fa ridge are more similar to the basaltic Troodos suite than to the MORB-like samples from the northern area. However, TiO_2 and FeO are higher and Al_2O_3 is lower in the Valu Fa samples than in Troodos basalt and appears intermediate in composition between Troodos basalt and that of the MORB-like basalt of the northern area. The Troodos lava is interpreted to have erupted in an incipient fore-arc setting (Robinson et al., 1983; Schmincke et al., 1983).

DISCUSSION AND CONCLUSIONS

Glass compositions of volcanic rocks dredged from Lau Basin show that lava erupted at a spreading center in the northern basin is distinct from that of Valu Fa Ridge, the spreading center in the southern basin. Glasses from the northern area resemble N-MORB but range from relatively primitive compositions to evolved ferrobasalt. The MORB-like glasses show narrow compositional trends compatible with olivine+plagioclase±clinopyroxene fractionation of parental magma generated from similar mantle sources. These glasses are similar to N-MORB from the Galapagos spreading center and to other oceanic spreading centers. Similar basalt compositions have previously been reported from Lau Basin by Hawkins (1976) and Hawkins and Melchior (1985), who reported that N-MORB compositions are restricted to the central area of the northern basin, whereas compositions near the margins of the basin are more arc-like. Hawkins and Melchior suggest this compositional zonation may reflect the evolution of the Lau Basin. Lava with arc-like characteristics erupts in the early stage of back-arc evolution due to the proximity of the arc. As spreading becomes established, the contribution from subducted crust, or metasomatized mantle, diminishes and MORB-like lava is erupted.

Glasses from Valu Fa Ridge, the southern spreading center, are predominantly andesite and minor basaltic andesite, which are distinct from andesite erupted at mid-ocean ridge spreading centers. Andesite from the Galapagos rift zone have higher TiO_2 and FeO, and lower Al_2O_3 content than comparably differentiated andesite from Valu Fa Ridge. However, Valu Fa andesite is higher in TiO_2, P_2O_5, and Na_2O than andesite typically erupted in island arcs (Gill, 1981) such as the

nearby Tofua arc (Ewart et al., 1973; Vallier et al., 1985). These glasses are rapidly quenched, volatile-rich lava that differentiated from parental magma intermediate in composition between an island arc and a MORB-like basalt. It is possible that andesitic lava erupted on Valu Fa Ridge represents the earlier stage of back-arc spreading, and may be followed by less fractionated basaltic lava when spreading becomes established and the ridge is no longer as close to the arc. The Lau Basin apparently opened by propagation of the spreading axis from north to south (Hawkins and Melchior, 1985), a trend reflected in the south-verging, wedge shape of the basin.

In the northern study area some older fractionated basaltic andesite was recovered on cruise SO-35-2 (von Stackelberg, 1985) similar to those reported by Hawkins and Melchior (1985) from the margins of the basin. However, these samples are not as differentiated and volatile-rich as many of the Valu Fa samples. Valu Fa Ridge andesite appears to have been generated from an exceptionally hydrous magma. Hydrous magma becomes over-saturated during ascent, resulting in boiling off of water, promoting crystallization, and hence differentiation (Gill, 1981). Vesiculation and degassing may have occurred within the magma chamber. The sill-like molten layer at the top of the magma chamber identified by Morton and Sleep (1985) may very well be the volatile-rich, most evolved layer in a compositionally stratified magma chamber. Oxygen fugacity would also be expected to be very high and possibly quite variable within different zones in the magma chamber, and result in variable TiO_2 content in titanomagnetite. The scatter in TiO_2 observed in Valu Fa andesite could be explained in this manner.

Volatile-rich, andesitic glasses that closely resemble Valu Fa andesite occur at the Troodos ophiolite (Robinson et al., 1983). This sequence grades upward into an Mg-rich basaltic island arc suite, and has been interpreted as an incipient fore-arc. It is possible that volatile-rich andesitic magma is erupted in the earliest stage of back- and fore-arc development. In the case of a back-arc, andesite is followed by less fractionated basaltic andesite and finally MORB-like basalt as spreading is established and the influence of subducted crust, or metasomatized mantle, is diminished.

REFERENCES

Bence, A.E., and Albee, A.L., 1968, Empirical correction factors for the electron microanalysis of silicates and oxides: J. Geol., v.76, p.382-404.

Byerly, G., 1980, The nature of differentiation trends in some volcanic rocks from the Galapagos spreading center: J. Geophys. Res., v.85, p.3797-3810.

Clague, D.A., Frey, F.A., Thompson, G., and Rindge, S., 1981, Minor and trace element geochemistry of volcanic rocks dredged from the Galapagos spreading center: Role of crystal fractionation and mantle heterogeneity: J. Geophys. Res., v.86, p.9469-9482.

Ewart, A., Bryan, W., and Gill, J., 1973, Mineralogy and geochemistry of the younger volcanic islands of Tonga: J. Petrol., v.14, p.429-466.

Fornari, D.J., Perfit, M.R., Malahoff, A., and Embley, R., 1983, Geochemical studies of abyssal lavas recovered by DSRV Alvin from eastern Galapagos Rift, Inca Transform and Ecuador Rift 1. Major element variations in natural glasses and spatial distribution of lavas: J. Geophys. Res., v.88, p.10,519-10,529.

Gill, J.B., 1981, Orogenic andesites and plate tectonics: Springer Verlag, Berlin, 390p.

Hawkins, J.W., 1976, Petrology and geochemistry of basaltic rocks from Lau Basin: Earth Plan. Sci. Lett., v.28, p.283-297.

Hawkins, J.W. and Melchior, J.T., 1985, Petrology of Mariana Trough and Lau Basin basalts: J. Geophys. Res., v. 90, p.11,431-11,468.

Jenner, G., Rautenschlein, M., Cawood, P., and White, W., 1985, Sr, Nd, and Pb isotopic composition and geochemistry of Valu Fa Ridge volcanics, Lau Basin: EOS Trans. AGU, v. 66, p.409.

Karig, D.E., 1971, Origin and development of marginal basins in the western Pacific: J. Geophys. Res., v.76, p.2542-2561.

Mathez, E.A., 1976, Sulfur solubility and magmatic sulfides in submarine glasses: J. Geophys. Res., v.81, p.4269-4276.

Moore, J.G., and Fabbi, B.P., 1971, An estimate of juvenile sulfur content of basalt: Contrib. Mineral. Petrol., v.33, p.118-127.

Morton, J.L. and Sleep, N.H., 1985, Seismic reflections from a Lau Basin magma chamber, in Scholl, D.W. and Vallier, T.L. (eds), Geology of Offshore Resources of Pacific Island Arcs-Tonga Region: Circum-Pacific Council for Energy and Mineral Resources, Earth Science Series, v. 2, p.441-453.

Robinson, P.T., Melson, W.G., O'Hearn, T., and Schmincke, H-U., 1983, Volcanic glass compositions of the Troodos ophiolite, Cyprus: Geology, v.11, p.400-404.

Schmincke, H.-U., Rautenschlein, M., Robinson, P.T., and Mehegan, J.M., 1983, Troodos extrusive series of Cyprus: A comparison with oceanic crust: Geology, v.11, p.405-409.

Vallier, T.L., Stevenson, A.J., and Scholl, D.W., 1985, Petrology of igneous rocks from Ata Island,

Kingdom of Tonga, in Scholl, D.W. and Vallier, T.L. (eds), Geology of Offshore Resources of Pacific Island Arcs-Tonga Region: Circum-Pacific Council for Energy and Mineral Resources, Earth Science Series, v. 2, p.441-453.

Vallier, T.L., Jenner, G., Frey, F., Hawkins, J.W., Gill, J., Morris, J., Cawood, P., Morton, J.L., Scholl, D.W., Herzer, R., Stevenson, A., and White,L., 1987, Petrogenesis of andesite from Valu Fa Ridge, a back-arc spreading center in Lau Basin: Geol. Soc. Am. Bull., (in press).

von Stackelberg, U., and shipboard party, 1985, Back Arc-hydrothermalismus des Lau Beckens und des Nord Fiji Beckens: Bundesanstalt fur Geowissenschaften und Rohstoffe, Bericht SO35-2/3, 74p.

Table 1: Dredge Locations

Dredge No.	Location (Lat.°S)	(Long.°W)	Water depth (m)
Northern Area			
SO35-2-2KD	18°34.35	176°23.40	2360-2290
SO35-2-9KD	18°39.84	176°26.74	2390-2370
SO35-2-10KD	18°40.43	176°22.30	2680-2420
SO35-2-8KD	18°40.44	176°28.43	2260-2270
SO35-2-25KD	18°42.68	175°43.83	2820-2700
SO35-2-52KD	18°45.76	176°24.08	2810-2720
SO35-2-49KD	18°45.76	176°24.08	2810-2720
SO35-2-62KD	18°48.25	176°32.80	2280-2300
SO35-2-61KD	18°51.63	176°33.39	2300-2280
Southern Area			
SO35-2-84KD	22°08.41	176°36.63	1700-1745
SO35-2-87KD	22°10.74	176°33.17	1730-1880
SO35-2-68KD	22°11.27	176°35.41	2240-2000
SO35-2-73KD	22°12.51	176°36.09	1750-1700
SO35-2-77KD	22°13.41	176°36.47	1700-1800
SO35-2-81KD	22°14.36	176°36.63	1680-1650
SO35-2-79KD	22°14.43	176°36.82	1625-1700
SO35-2-127KD	22°14.44	176°36.91	1820-1680
SO35-2-83KD	22°14.74	176°36.92	1750-1715
SO35-2-72KD	22°15.36	176°37.33	1820-1620
SO35-2-71KD	22°17.06	176°37.33	1820-1620
L3-84-SP-D1	22°18.92	176°39.01	2063-1965
SO35-2-90KD	22°19.50	176°39.35	1870-1890
L3-84-SP-D2	22°19.89	176°39.37	1930-1875
SO35-2-91KD	22°20.51	176°39.39	1855-1880
SO35-2-94KD	22°23.35	176°40.82	1990-1920
SO35-2-97KD	22°32.08	176°42.68	1900-1920

Table 2: Microprobe Analyses of Volcanic Glasses Dredged from the Southern Study Area in Lau Basin on cruise L3-84-SP

Sample No.	D1c	D1d	D1-12	D1-83	D1-10	D1-11	D1-9	D1a	D1b	D1-8	D2-15	D2-7	D2-20	D2-2	D2b	D2a	D2-1	D2-6	D2-27	D2c
(wt.%)																				
SiO_2	55.1	55.3	56.8	57.1	56.9	56.7	57.1	57.5	57.4	57.3	54.4	54.6	54.6	54.5	54.7	54.5	54.8	54.8	55.1	56.8
Al_2O_3	14.9	14.8	13.8	13.3	13.6	14.6	14.3	14.5	14.8	15.1	14.4	13.8	13.5	13.7	13.7	13.9	15.1	16.1	13.0	15.5
FeO^T	10.5	10.4	12.0	11.8	11.7	11.2	11.2	9.89	10.0	10.9	11.8	13.0	12.9	12.6	12.9	13.0	11.8	11.4	12.8	10.6
MnO	0.18	0.18	0.20	0.22	0.20	0.20	0.20	0.18	0.19	0.19	0.20	0.21	0.23	0.20	0.20	0.20	0.19	0.19	0.19	0.19
MgO	3.79	3.75	2.89	2.77	2.77	2.70	2.65	2.60	2.53	2.25	3.83	3.49	3.37	3.35	3.30	3.19	3.00	2.96	2.92	2.79
CaO	7.91	7.99	7.04	6.83	6.88	7.37	7.14	6.79	6.79	7.11	8.17	7.52	7.64	7.73	7.65	7.58	7.94	8.18	7.63	7.40
Na_2O	3.14	3.12	2.66*	3.32	3.25	3.40	3.31	3.46	3.53	3.62	3.02	2.27*	3.05	3.11	3.08	3.00	3.22	3.30	2.43*	3.45
K_2O	0.42	0.40	0.47	0.50	0.48	0.45	0.46	0.44	0.46	0.50	0.38	0.42	0.41	0.40	0.39	0.42	0.37	0.37	0.43	0.40
P_2O_5	0.20	0.16	0.19	0.22	0.23	0.17	0.20	0.27	0.20	0.17	0.15	0.21	0.23	0.22	0.19	0.20	0.15	0.15	0.18	0.16
TiO_2	1.29	1.28	1.67	1.61	1.57	1.52	1.53	1.56	1.59	1.49	1.38	1.75	1.76	1.76	1.79	1.82	1.62	1.58	1.86	1.50
Total	97.4	97.4	97.7	97.7	97.6	98.3	98.1	97.2	97.5	98.7	97.7	97.3	97.6	97.5	97.9	97.7	98.1	99.0	96.6	98.7
S (ppm)	140	130	160	140	110	160	150	150	150	130	120	190	170	170	220	150	170	170	380	120
CIPW Normative Mineralogy ----- volatile-free																				
Q	9.53	8.56	15.7	13.5	13.9	11.7	13.1	14.4	13.5	11.9	8.40	13.4	9.84	9.55	9.86	10.1	9.25	8.27	14.6	11.3
Or	2.55	2.39	2.85	3.03	2.92	2.70	2.77	2.67	2.79	2.99	2.29	2.55	2.48	2.42	2.35	2.53	2.23	2.21	2.63	2.39
Ab	27.3	26.6	23.1	28.8	28.3	29.2	28.5	30.1	30.6	31.0	26.1	19.7	26.4	27.0	26.6	25.9	27.7	28.2	21.3	29.5
An	26.0	25.5	25.0	20.4	21.7	23.6	23.1	23.4	23.8	23.8	25.1	27.0	22.4	22.8	22.8	23.6	26.0	28.2	24.2	25.8
DiWo	5.40	5.62	3.99	5.36	4.94	5.16	4.87	3.91	3.90	4.48	6.38	4.14	6.21	6.27	6.10	5.62	5.48	4.93	5.76	4.27
DiEn	2.15	2.04	1.28	1.68	1.59	1.63	1.52	1.32	1.29	1.28	2.37	1.40	2.07	2.12	2.01	1.81	1.80	1.64	1.78	1.43
DiFs	3.30	3.70	2.85	3.88	3.52	3.72	3.53	2.70	2.73	3.41	4.13	2.86	4.34	4.34	4.29	4.01	3.86	3.44	4.21	2.98
HyEn	7.54	7.38	6.09	5.39	5.51	5.20	5.20	5.33	5.17	4.39	7.37	7.52	6.52	6.42	6.37	6.31	5.81	5.80	5.75	5.60
HyFs	11.5	13.4	13.5	12.5	12.2	11.9	12.1	10.9	11.0	11.7	12.9	15.4	13.7	13.1	13.6	14.0	12.5	12.1	13.6	11.7
Mt	1.73	1.96	1.95	1.93	1.85	1.84	1.85	1.64	1.65	1.78	1.95	2.14	2.14	2.08	2.11	2.13	1.93	1.86	2.13	1.73
Il	2.52	2.45	3.25	3.13	3.07	2.93	2.96	3.04	3.09	2.86	2.68	3.41	3.42	3.42	3.47	3.53	3.13	3.03	3.65	2.88
Ap	0.49	0.38	0.46	0.53	0.56	0.41	0.48	0.66	0.49	0.41	0.36	0.51	0.56	0.53	0.50	0.48	0.36	0.36	0.44	0.38

Note: for norm calculations FeO=0.9FeO total (FeO^T)

* low Na_2O values

Table 3: Microprobe Analyses of Volcanic Glasses Dredged from the Northern Study Area in Lau Basin on Cruise SO35-2

Sample No.	2KDB	9KDA	10KDA	8KDA	25KD	52KD	49KDB	62KD	61KD
(wt.%)									
SiO_2	50.3	50.1	48.9	50.5	48.2	51.1	50.4	50.3	49.9
Al_2O_3	14.4	14.3	15.2	14.3	15.7	13.6	13.4	13.9	13.8
FeO^T	11.1	10.8	10.7	11.2	9.64	12.4	13.8	12.4	12.6
MnO	0.19	0.19	0.20	0.18	0.18	0.22	0.24	0.21	0.23
MgO	7.20	7.40	8.15	7.52	9.14	6.28	6.03	6.97	6.80
CaO	11.6	12.1	12.0	11.7	11.8	10.5	10.3	11.0	10.8
Na_2O	2.66	2.67	2.60	2.65	2.67	3.16	3.09	2.80	2.82
K_2O	0.09	0.05	0.03	0.06	0.06	0.16	0.08	0.06	0.08
P_2O_5	0.09	0.05	0.05	0.06	0.04	0.17	0.07	0.04	0.08
TiO_2	1.41	1.23	1.26	1.24	1.12	1.66	1.88	1.42	1.61
Total	99.0	98.9	99.1	99.4	98.6	99.3	99.3	99.1	98.7
S (ppm)	920	1080	1130	1160	880	1210	1260	1230	1100
CIPW Normative Mineralogy --- volatile-free									
Or	0.54	0.30	0.18	0.36	0.36	0.95	0.48	0.36	0.48
Ab	22.7	22.8	22.2	22.5	22.9	26.9	26.3	23.9	24.1
An	27.3	27.1	29.8	27.1	31.0	22.7	22.5	25.3	25.1
DiWo	12.5	13.9	12.5	12.9	11.8	12.0	11.9	12.4	11.9
DiEn	6.52	7.41	6.92	6.78	7.02	5.67	5.25	6.06	5.76
DiFs	5.59	6.08	5.10	5.72	4.18	6.13	6.59	6.10	5.97
HyEn	8.89	6.45	3.84	8.23	0.72	8.61	7.82	8.07	7.99
HyFs	7.62	5.29	2.83	6.94	0.43	9.31	9.81	8.13	8.28
OlFo	1.87	3.34	6.81	2.67	10.7	1.03	1.43	2.35	2.36
OlFa	1.77	3.02	5.54	2.48	7.04	1.23	1.97	2.61	2.69
Mt	1.81	1.76	1.74	1.82	1.57	2.00	2.25	2.02	2.05
Il	2.70	2.36	2.41	2.37	2.16	3.17	3.59	2.72	3.09
Ap	0.22	0.12	0.12	0.14	0.10	0.41	0.17	0.10	0.19

Note: for norm calculations FeO=0.9 FeO total (FeO^T)

Table 4: Microprobe Analyses of Volcanic Glasses Dredged from the Southern Study Area in Lau Basin on Cruise SO35-2

Sample No.	84KD	87KD	68KD	73KD	77KD	81KD	79KD	127KD	83KD	72KD	71KD	90KDB	91KDB	94KDB	97KDK
(wt.%)															
SiO_2	52.3	52.1	52.2	57.7	58.0	60.0	58.9	56.0	56.3	59.6	58.3	55.2	54.3	56.5	54.3
Al_2O_3	13.5	14.3	14.6	14.5	14.3	13.6	14.1	13.8	15.3	13.7	14.9	14.3	14.5	14.6	14.5
FeO^T	11.2	12.0	9.35	9.76	10.1	9.48	9.41	10.7	10.3	9.72	9.52	11.2	12.3	10.0	11.7
MnO	0.20	0.22	0.17	0.20	0.19	0.19	0.19	0.20	0.20	0.20	0.20	0.20	0.20	0.18	0.19
MgO	5.66	5.70	6.07	2.33	2.60	2.22	2.34	3.15	3.02	2.25	2.29	3.40	3.54	2.81	3.70
CaO	10.2	10.2	10.9	6.69	6.57	6.32	6.20	7.15	7.63	6.19	6.34	7.32	7.60	7.53	7.82
Na_2O	2.20	1.77	2.41	3.34	3.32	3.24	3.55	3.31	3.57	3.27	3.55	3.34	3.08	3.28	3.21
K_2O	0.26	0.39	0.24	0.51	0.50	0.56	0.55	0.45	0.41	0.57	0.51	0.41	0.41	0.42	0.36
P_2O_5	0.11	0.05	0.08	0.28	0.28	0.28	0.28	0.22	0.16	0.28	0.28	0.21	0.16	0.21	0.16
TiO_2	1.16	0.83	0.97	1.56	1.66	1.50	1.40	1.56	1.39	1.55	1.46	1.62	1.58	1.62	1.49
Total	96.8	97.5	97.0	96.9	97.6	97.4	97.0	96.5	98.3	97.3	97.3	97.2	97.7	97.2	97.5
S (ppm)	100	30	260	120	200	160	160	280	130	100	140	230	280	240	340
CIPW Normative Mineralogy ------ volatile-free															
Q	5.97	7.15	4.53	15.3	16.3	18.9	16.5	12.3	9.21	18.9	15.4	9.15	10.8	11.5	8.96
Or	1.57	2.38	1.46	3.10	3.05	3.37	3.35	2.76	2.44	3.46	3.09	2.46	2.54	2.50	2.20
Ab	19.1	15.5	21.0	29.1	29.0	27.9	30.9	29.1	30.4	28.4	30.8	28.7	27.3	28.0	28.1
An	26.8	31.0	29.2	23.7	23.4	21.2	21.7	22.1	24.7	21.5	23.8	23.0	25.7	24.2	25.0
DiWo	10.1	8.69	10.8	3.57	3.46	3.71	3.40	5.50	5.17	3.43	2.75	5.20	5.32	5.08	5.87
DiEn	4.54	3.98	5.61	1.12	1.22	1.10	1.10	2.00	1.73	1.07	0.88	1.78	2.13	1.60	2.29
DiFs	5.53	4.64	4.94	2.59	2.32	2.77	2.42	3.62	3.59	2.49	1.97	3.57	3.24	3.67	3.65
HyEn	9.89	10.7	9.96	4.85	5.45	4.53	4.90	6.14	5.84	4.68	4.98	6.82	7.10	5.46	7.25
HyFs	12.1	12.4	8.78	11.3	10.4	11.4	10.8	11.1	12.1	10.9	11.2	13.7	10.8	12.5	11.5
Mt	1.97	1.87	1.55	1.67	1.57	1.70	1.57	1.76	1.81	1.61	1.58	2.02	1.69	1.90	1.79
Il	2.25	1.63	1.90	3.05	3.25	2.90	2.74	3.07	2.66	3.02	2.85	3.13	3.14	3.11	2.93
Ap	0.27	0.12	0.20	0.68	0.68	0.68	0.68	0.54	0.38	0.68	0.68	0.51	0.40	0.50	0.39

Note: for no. m calculations FeO=0.9 FeO total (FeO^T)

FIGURE CAPTIONS

Figure 1. Map showing location of two spreading centers in Lau Basin. Study areas are enclosed in boxes. (from von Stackelberg and shipboard party, 1985).

Figure 2. Bathymetry and dredge locations in the northern study area. Bathymetric map modified from Chase et al. (1985).

Figure 3. Bathymetry and dredge locations in the southern study area. Location of seismic lines 10 and 11 (Morton and Sleep, 1985) are indicated by dashed lines. Bathymetric map modified from Chase et al. (1985).

Figure 4. SiO_2 (a) and Al_2O_3 (b) vs. MgO variation diagrams of glass compositions from two spreading centers in Lau Basin. Samples from the northern center are shown as circles, whereas samples from Valu Fa Ridge, the southern center, are shown by triangles. The island arc basalt (87KD) dredged from the eastern flank of Valu Fa Ridge is shown as a filled triangle. Galapagos and Ecuador Rift and Troodos ophiolite glass compositions shown for comparison are shown as fields. SiO_2 contents are similar for all except the basaltic suite from Troodos, which has higher SiO_2 at a given MgO. Al_2O_3 content of samples from the northern spreading center in Lau Basin are very similar to those from the Equador Rift, but Al_2O_3 of andesitic glasses from Valu Fa Ridge are much higher than comparably evolved Galapagos Rift samples. Data from East Pacific mid-ocean ridge spreading centers from Byerly, (1980), and Fornari et al., (1983); data from Troodos ophiolite from Robinson et al., (1983).

Figure 5. (a) CaO vs. MgO variatian diagram shows a similar range in CaO for Lau Basin samples as that of comparably evolved Galapagos or Troodos samples. (b) Na_2O of Lau Basin samples is slightly higher and shows a larger compositional range than Galapagos samples, but the andesitic samples are generally similar to those from Troodos. Symbols and data sources as in figure 4.

Figure 6. (a) K_2O vs. MgO variation diagram shows very similar compositions for samples from the northern Lau Basin compared with East Pacific spreading centers. Andesitic samples from Valu Fa Ridge are similar to Galapagos and Troodos andesite but the Troodos andesite suite shows a much larger range in K_2O. (b) P_2O_5 vs. MgO also shows the same range in composition for northern Lau Basin samples and East Pacific mid-ocean ridge spreading centers, but the andesitic samples from Valu Fa Ridge are considerably lower in P_2O_5 than comparably evolved Galapagos andesite. P_2O_5 data for Troodos glasses was not available. Symbols and data sources as in figure 4.

Figure 7. FeO^T (a) and TiO_2 (b) vs. MgO variation diagrams show that samples from the northern Lau Basin are very similar to those from Galapagos and Ecuador Rifts. Andesitic samples of Valu Fa Ridge are much lower in TiO_2 and FeO^T than Galapagos andesites, but are very similar to the andesitic suite of the Troodos ophiolite. However, the three less fractionated samples from Valu Fa Ridge appear intermediate in composition between the East Pacific mid-ocean ridge spreading centers and the Troodos basaltic suite. Symbols and data sources as in figure 4.

Figure 8. S vs. MgO (a) and S vs. FeO^T (b) variation diagrams of Lau Basin glasses show the northern samples undegassed and positively correlated with FeO content. Samples from

Valu Fa Ridge are low in S and appear degassesd but show no trend with MgO or FeO. Symbols same as in figure 4.

Figure 9. P_2O_5 vs. K_2O (a) and TiO_2 vs. K_2O (b) variation diagrams show a well-defined trend for samples from the northern area suggestive of a similar mantle source. Samples from Valu Fa Ridge show a considerable range in P_2O_5 and TiO_2 for a given K_2O content, suggesting that multiple differentiation trends involving titanomagnetite and different sources may have been involved. The island arc basalt is distinctively different from both the MORB-like samples from the northern spreading center and from the basaltic andesite of Valu Fa Ridge. Symbols as in figure 4. Trend of Galapagos lava at 85° and 95° W from Clague et al., (1981).

Figure 10. Compositional trends of (a) SiO_2, (b) MgO, and (c) K_2O vs. latitude of glasses from the southern study area show the most evolved composition and the greatest range in composition at about latitude 22°14' S with compositions becoming less fractionated both north and southward. Width of magma chamber determined by seismic lines 10 and 11 (Morton and Sleep, 1985) and positions of seismic lines and of offset at 22°12'S are indicated by dashed lines. Symbols as in figure 4. Range of compositions for L3-84 D1 and D2 are shown by tie-lines.

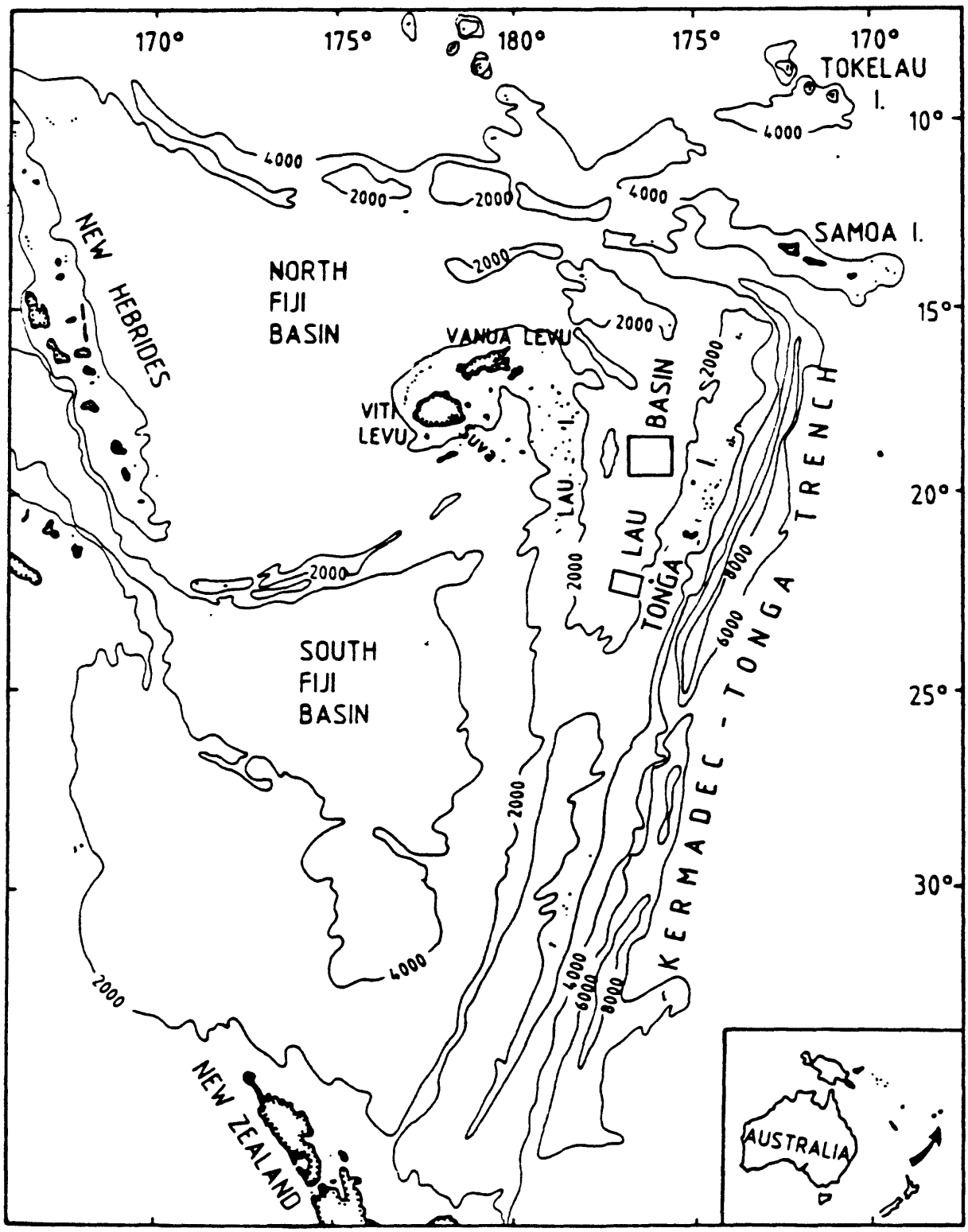
170°
175°
180°
175°
170°
TOKELAU I.
10°
15°
20°
25°
30°
SAMOA I.
NEW HEBRIDES
NORTH FIJI BASIN
VANUA LEVU
VITI LEVU
LAU
LAU BASIN
TONGA I.
KERMADEC - TONGA TRENCH
SOUTH FIJI BASIN
NEW ZEALAND
AUSTRALIA
2000
4000
6000
8000

Figure 1

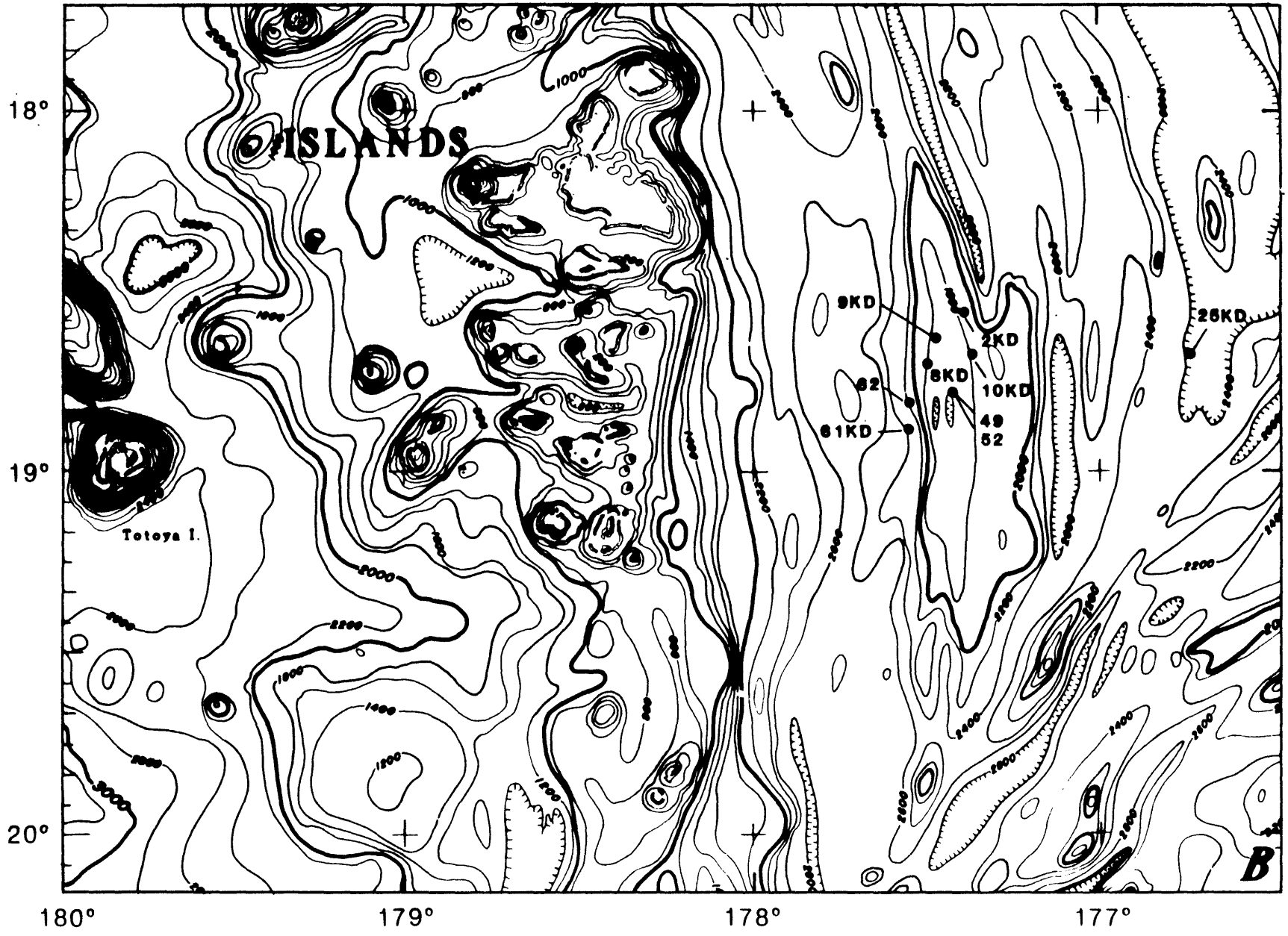
ISLANDS
Totoya I.
9KD
2KD
8KD
10KD
62
61KD
49
52
26KD
B
18°
19°
20°
180°
179°
178°
177°

Figure 2

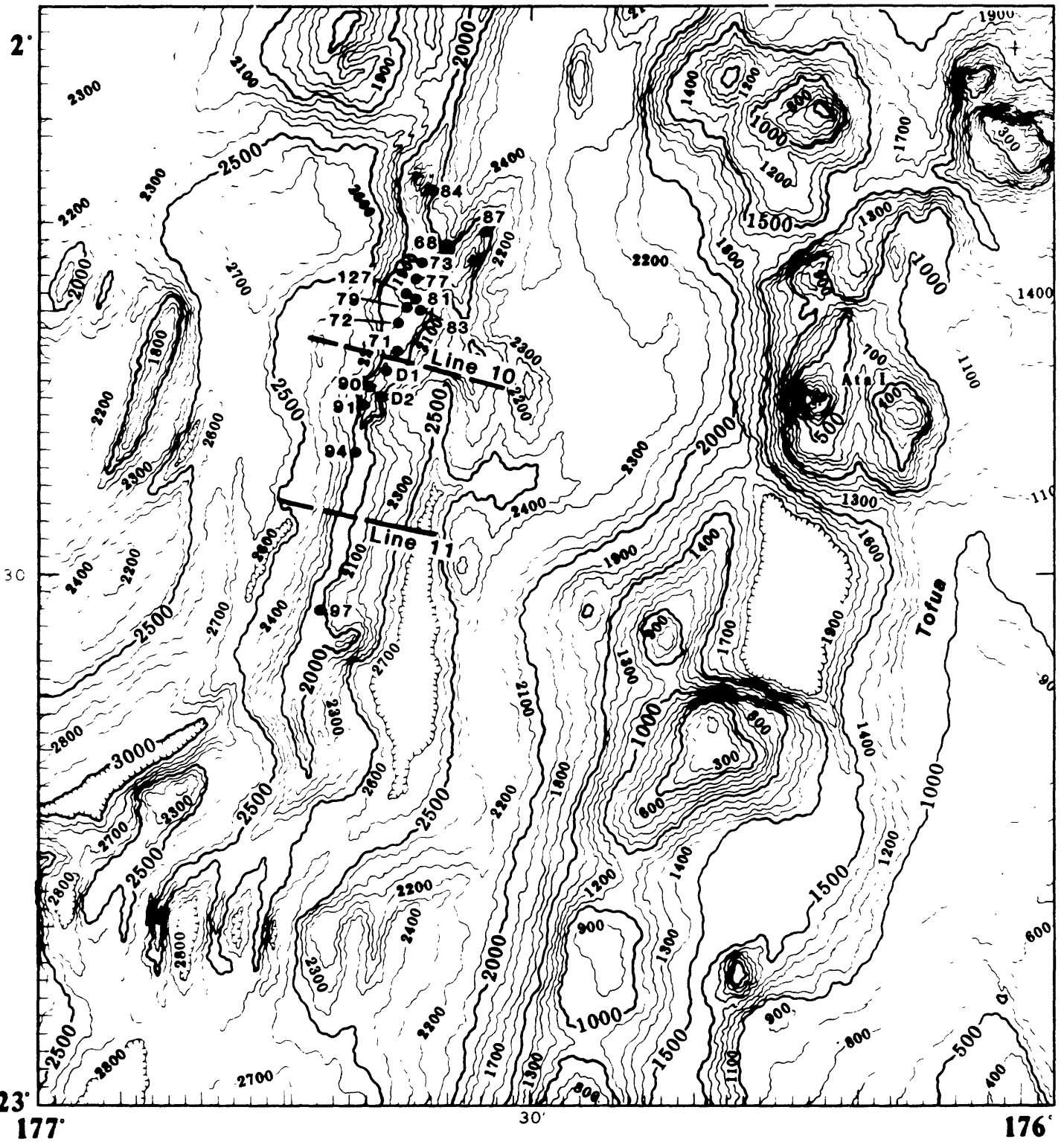
2°
30
23°
177°
30'
176°
Line 10
Line 11
D1
D2
Ata I
Tofua
84
87
68
73
77
127
79
81
72
83
71
90
91
94
97

Figure 3

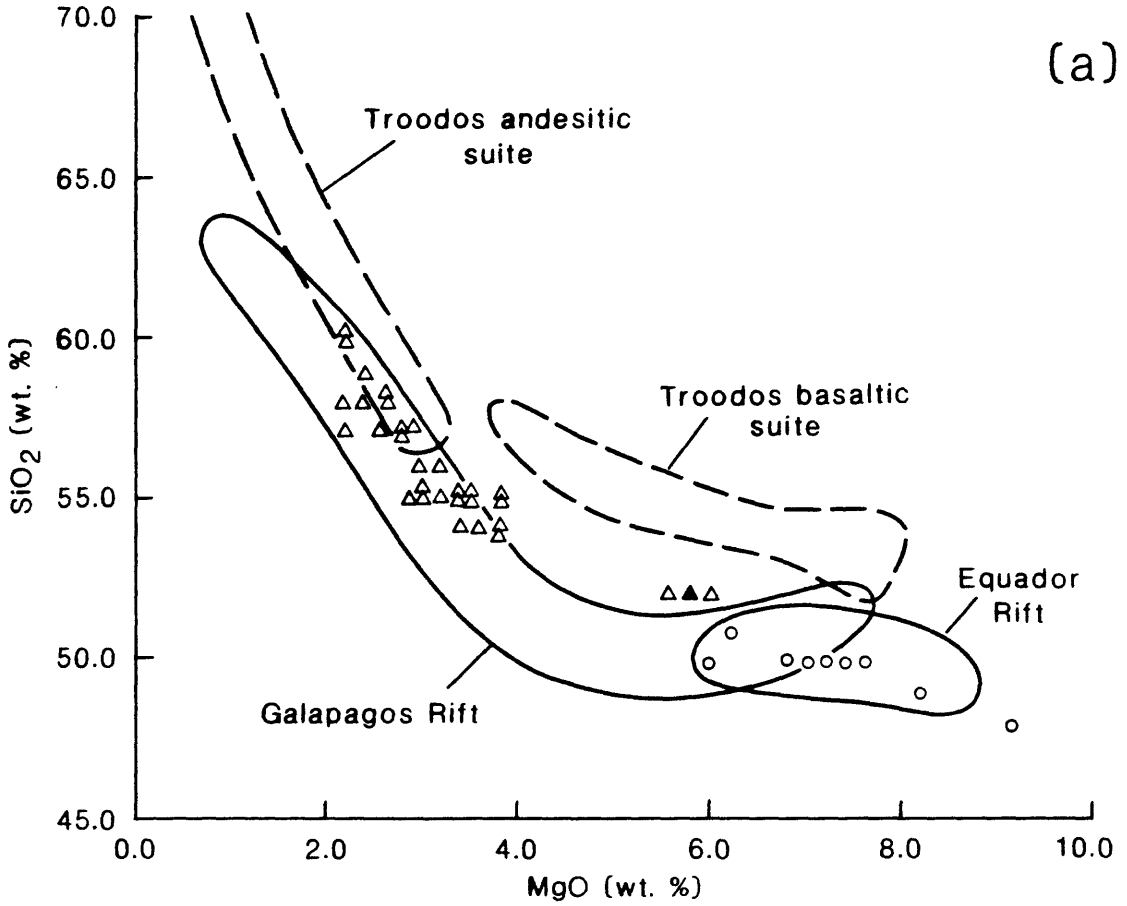
(a)
Troodos andesitic suite
Troodos basaltic suite
Equador Rift
Galapagos Rift
SiO_2 (wt. %)
MgO (wt. %)
70.0
65.0
60.0
55.0
50.0
45.0
0.0
2.0
4.0
6.0
8.0
10.0

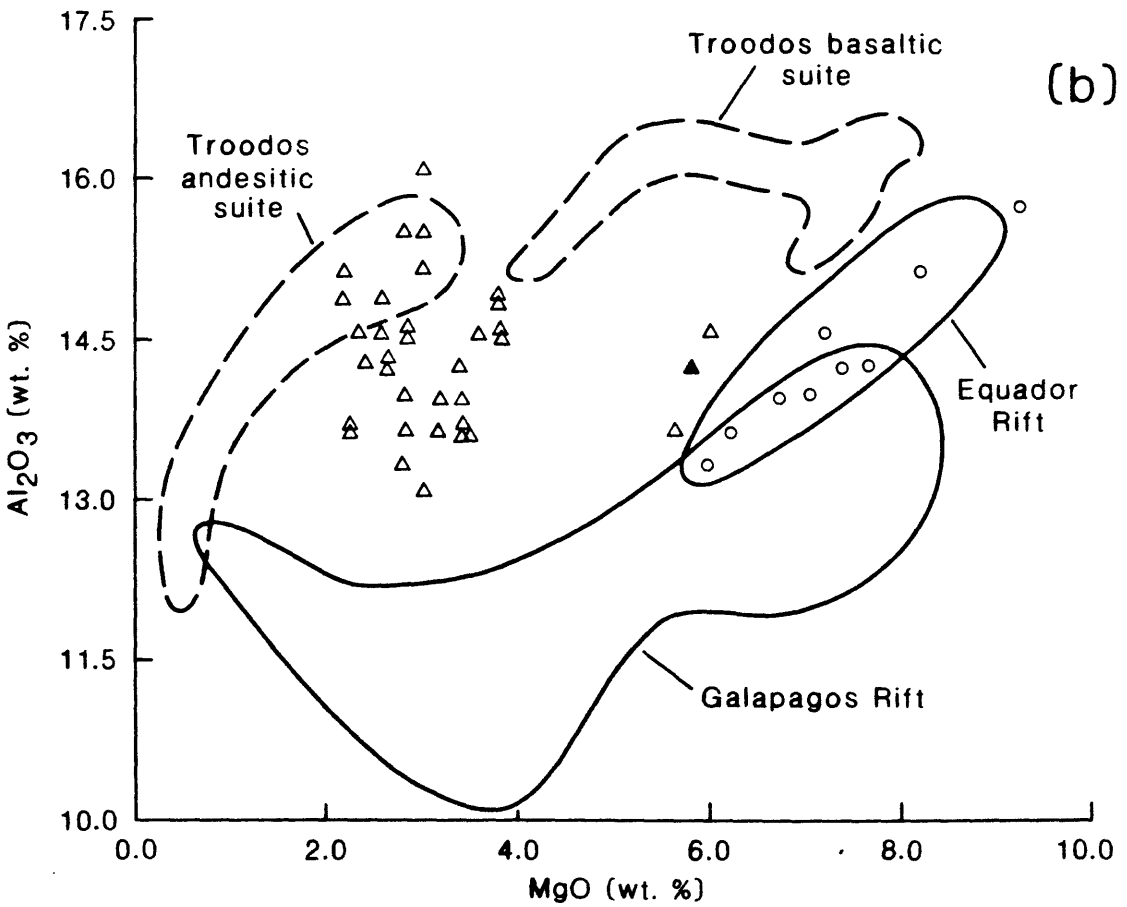
(b)
Troodos basaltic suite
Troodos andesitic suite
Equador Rift
Galapagos Rift
Al_2O_3 (wt. %)
MgO (wt. %)
17.5
16.0
14.5
13.0
11.5
10.0
0.0
2.0
4.0
6.0
8.0
10.0

Figure 4

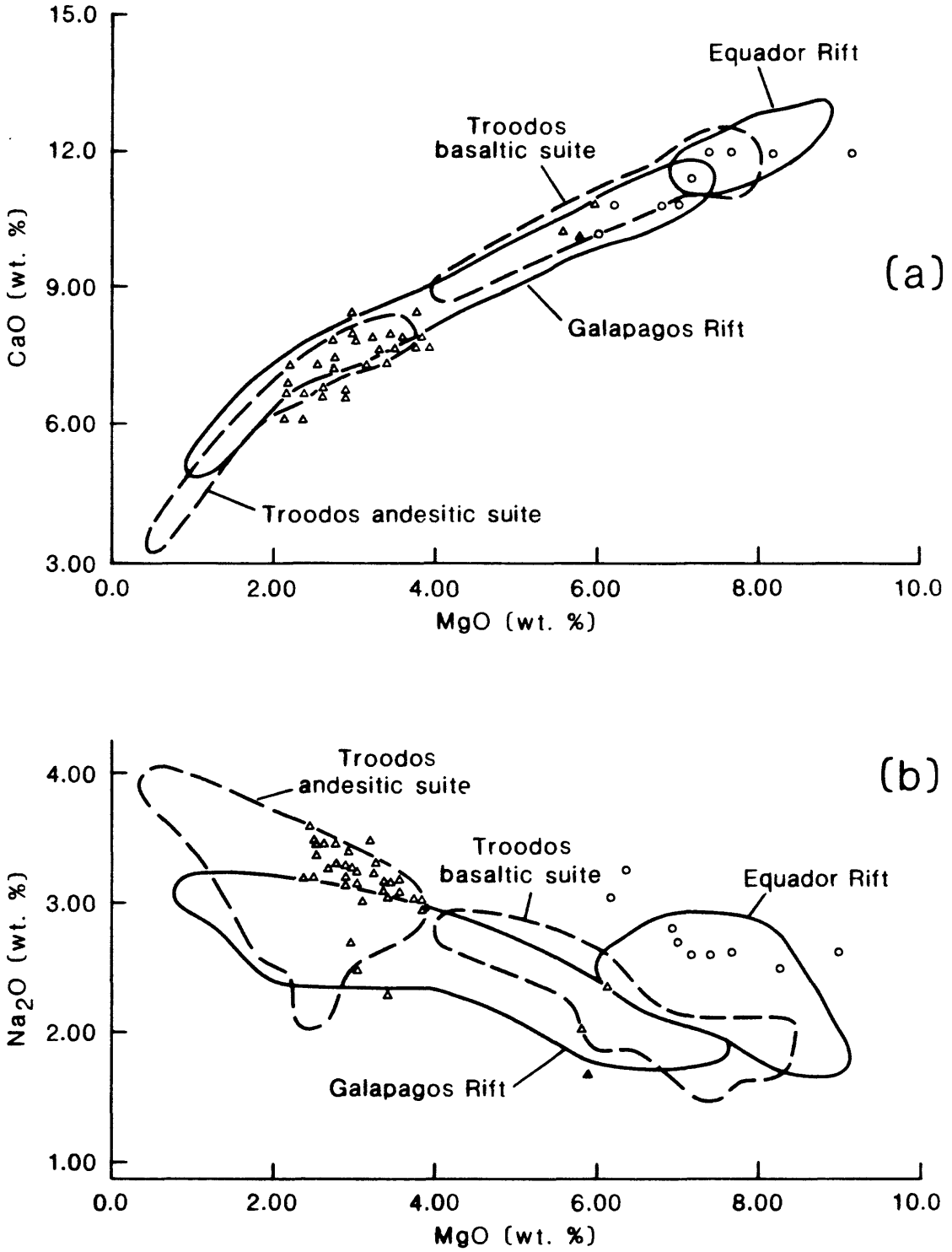
15.0
12.0
9.00
6.00
3.00
CaO (wt. %)
0.0
2.00
4.00
6.00
8.00
10.0
MgO (wt. %)
Equador Rift
Troodos
basaltic suite
Galapagos Rift
Troodos andesitic suite
(a)
4.00
3.00
2.00
1.00
Na_2O (wt. %)
Troodos
andesitic suite
Troodos
basaltic suite
Equador Rift
Galapagos Rift
(b)

Figure 5

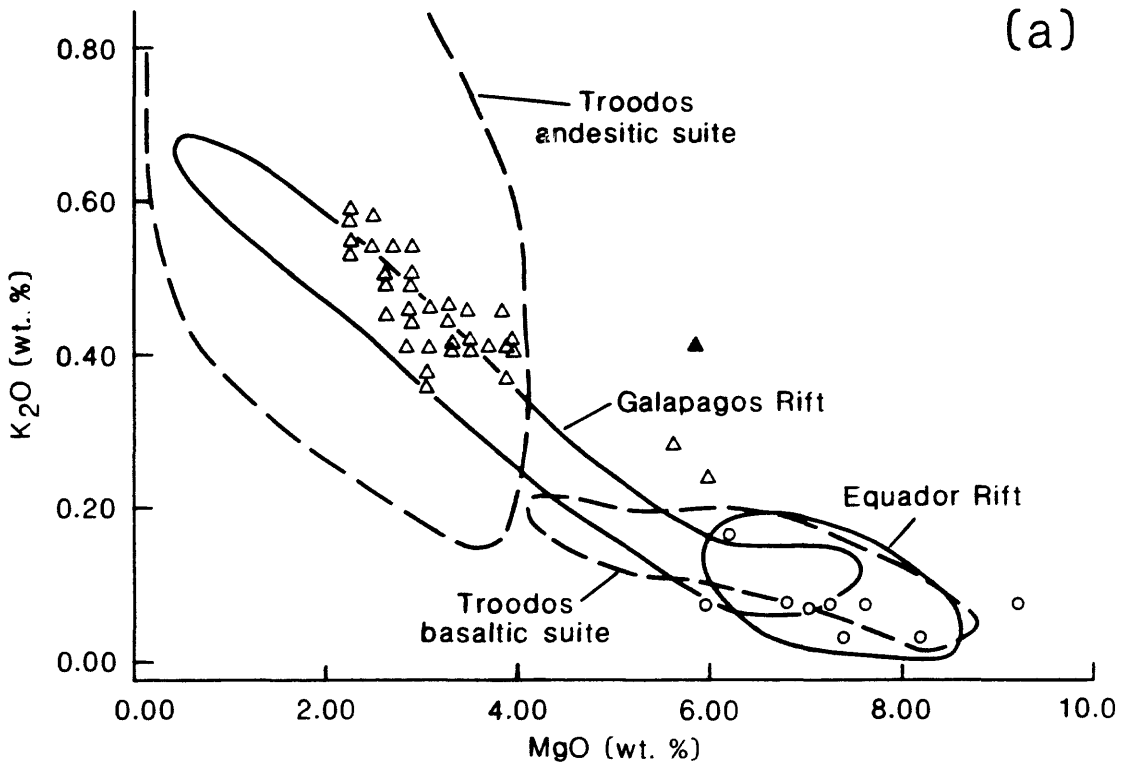
(a)
Troodos
andesitic suite
Galapagos Rift
Equador Rift
Troodos
basaltic suite
K_2O (wt. %)
MgO (wt. %)
0.00
0.20
0.40
0.60
0.80
0.00
2.00
4.00
6.00
8.00
10.0

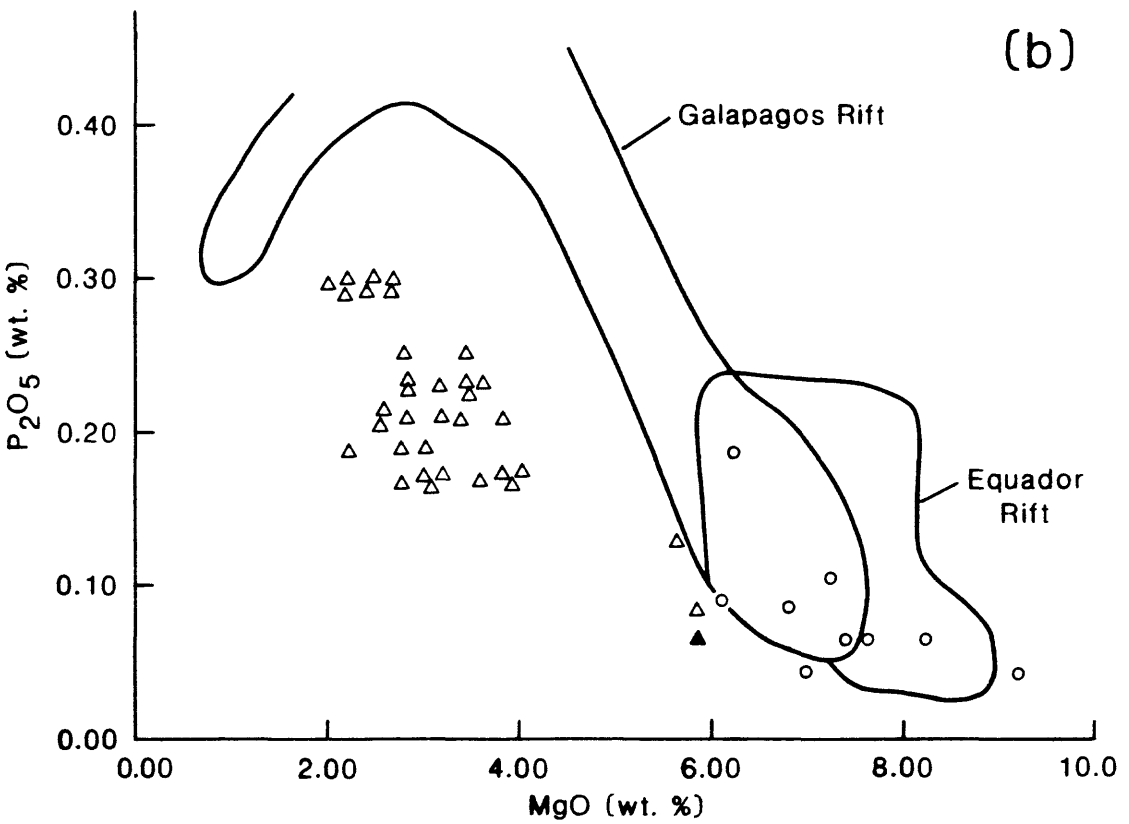
(b)
Galapagos Rift
Equador
Rift
P_2O_5 (wt. %)
MgO (wt. %)
0.00
0.10
0.20
0.30
0.40
0.00
2.00
4.00
6.00
8.00
10.0

Figure 6

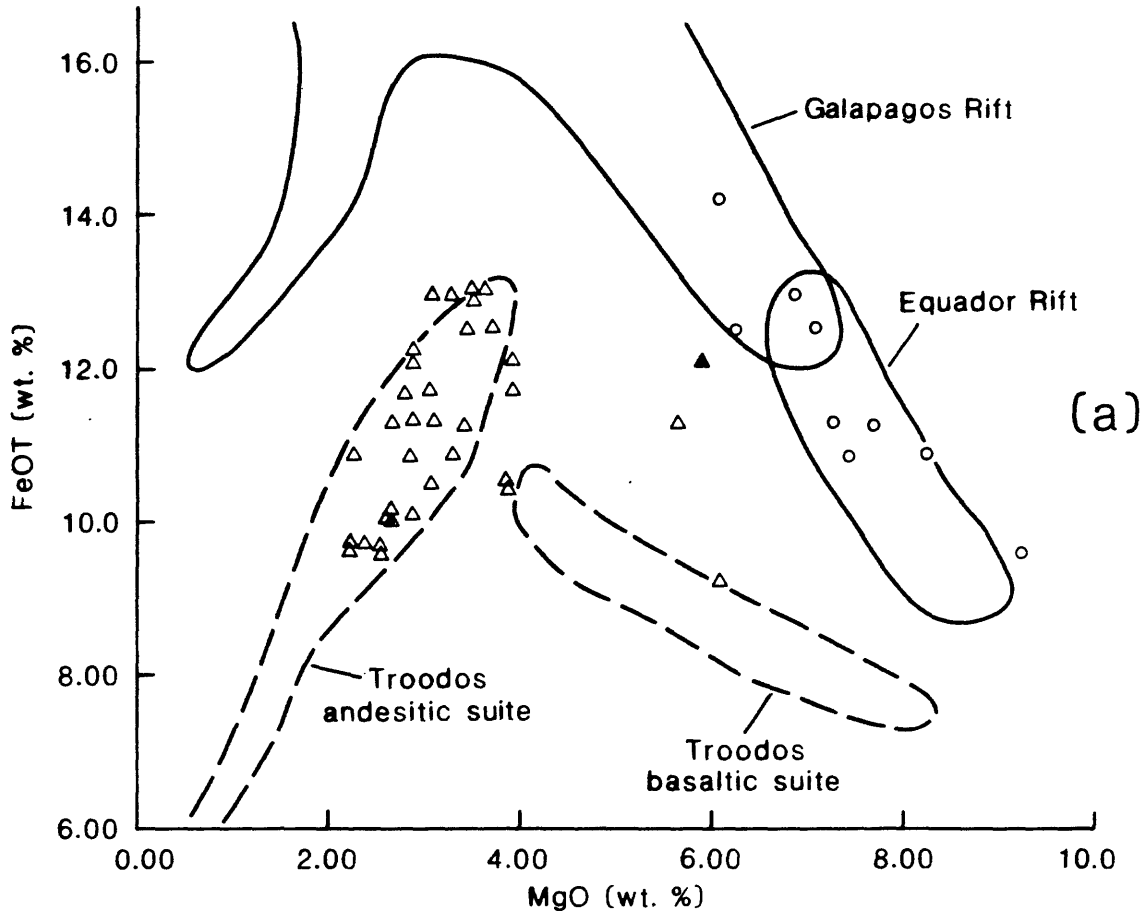
16.0
14.0
12.0
10.0
8.00
6.00
FeOT (wt. %)
0.00
2.00
4.00
6.00
8.00
10.0
MgO (wt. %)
Galapagos Rift
Equador Rift
(a)
Troodos
andesitic suite
Troodos
basaltic suite

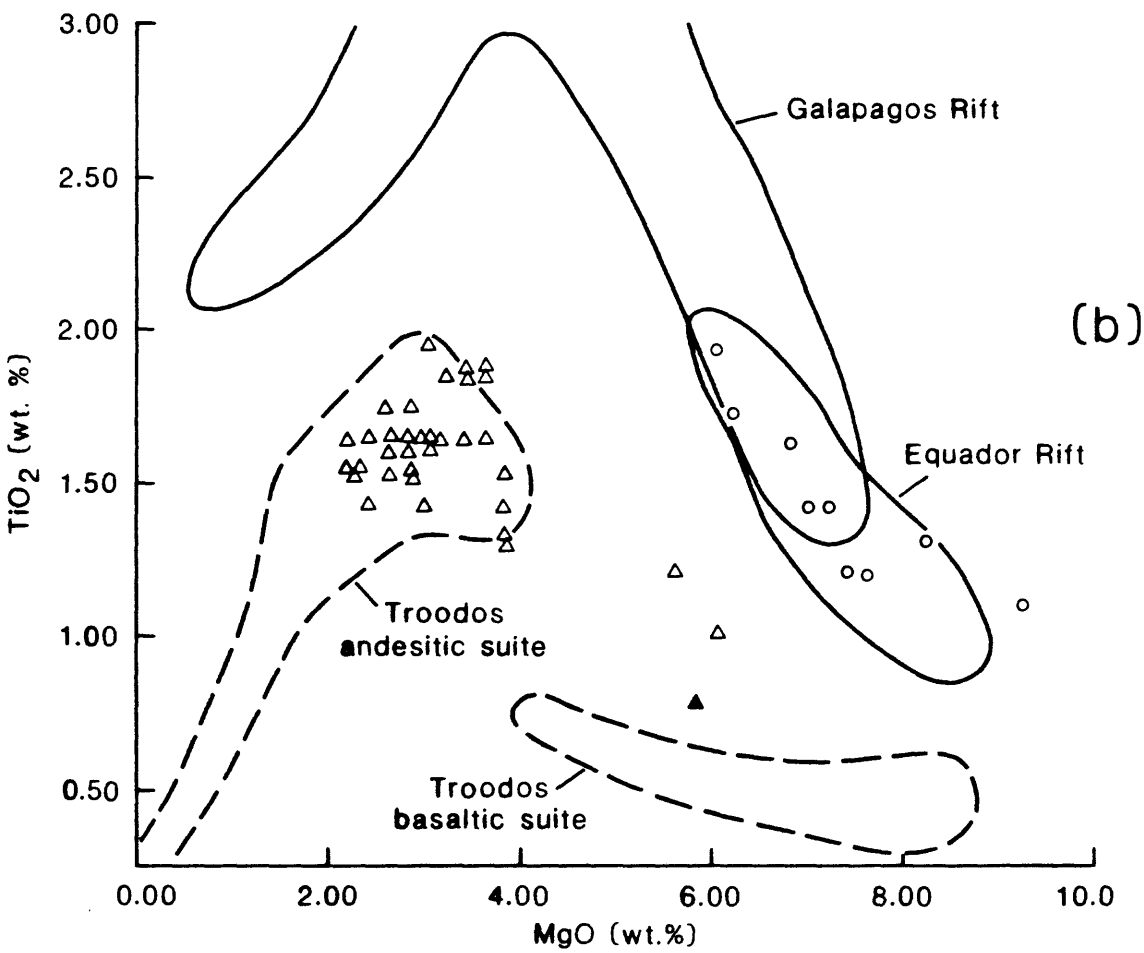
3.00
2.50
2.00
1.50
1.00
0.50
TiO2 (wt. %)
0.00
2.00
4.00
6.00
8.00
10.0
MgO (wt.%)
Galapagos Rift
(b)
Equador Rift
Troodos
andesitic suite
Troodos
basaltic suite

Figure 7

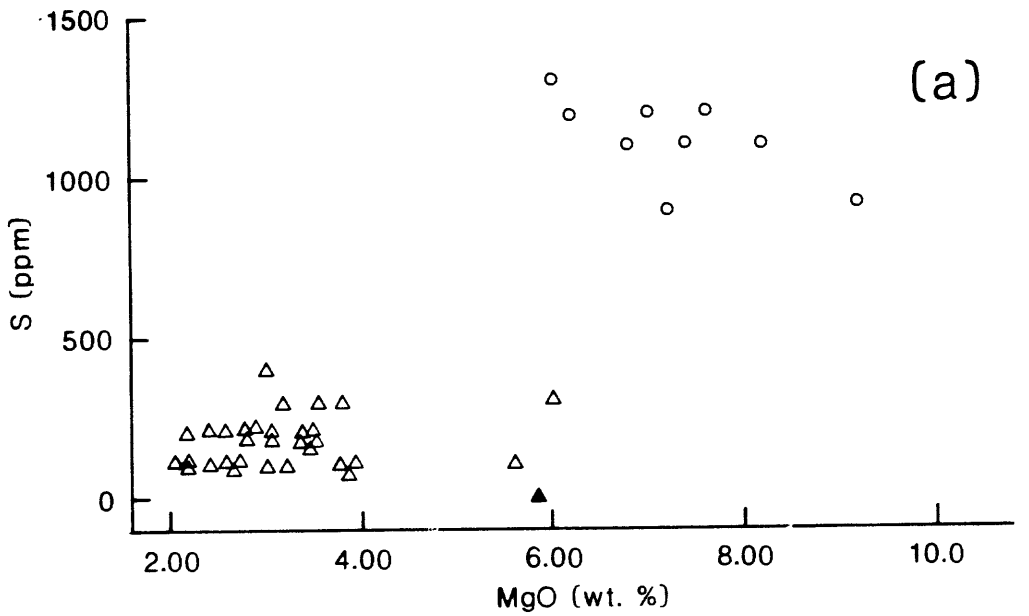
(a)
1500
1000
500
0
S (ppm)
2.00
4.00
6.00
8.00
10.0
MgO (wt. %)

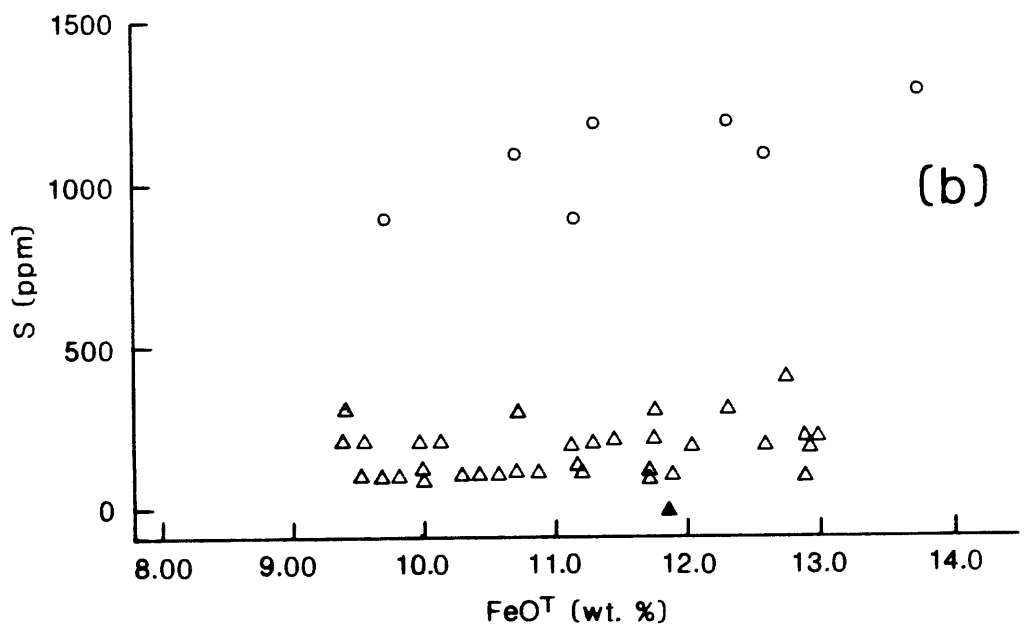
(b)
1500
1000
500
0
S (ppm)
8.00
9.00
10.0
11.0
12.0
13.0
14.0
FeO^T (wt. %)

Figure 8

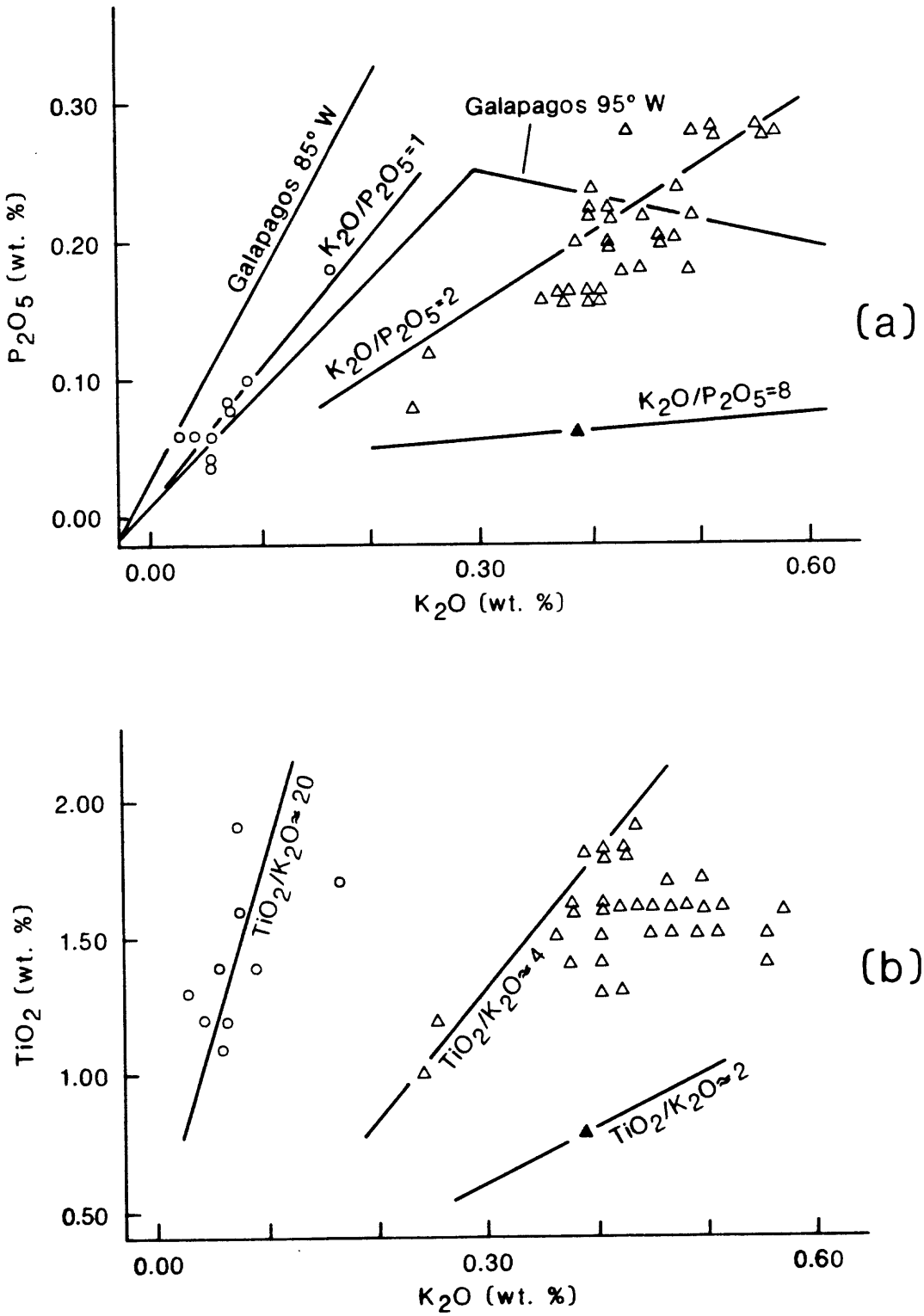
0.30
0.20
0.10
0.00
P_2O_5 (wt. %)
Galapagos 85° W
$K_2O/P_2O_5=1$
Galapagos 95° W
$K_2O/P_2O_5=2$
$K_2O/P_2O_5=8$
(a)
0.00
0.30
0.60
K_2O (wt. %)
2.00
1.50
1.00
0.50
TiO_2 (wt. %)
$TiO_2/K_2O \approx 20$
$TiO_2/K_2O \approx 4$
$TiO_2/K_2O \approx 2$
(b)
0.00
0.30
0.60
K_2O (wt. %)

Figure 9

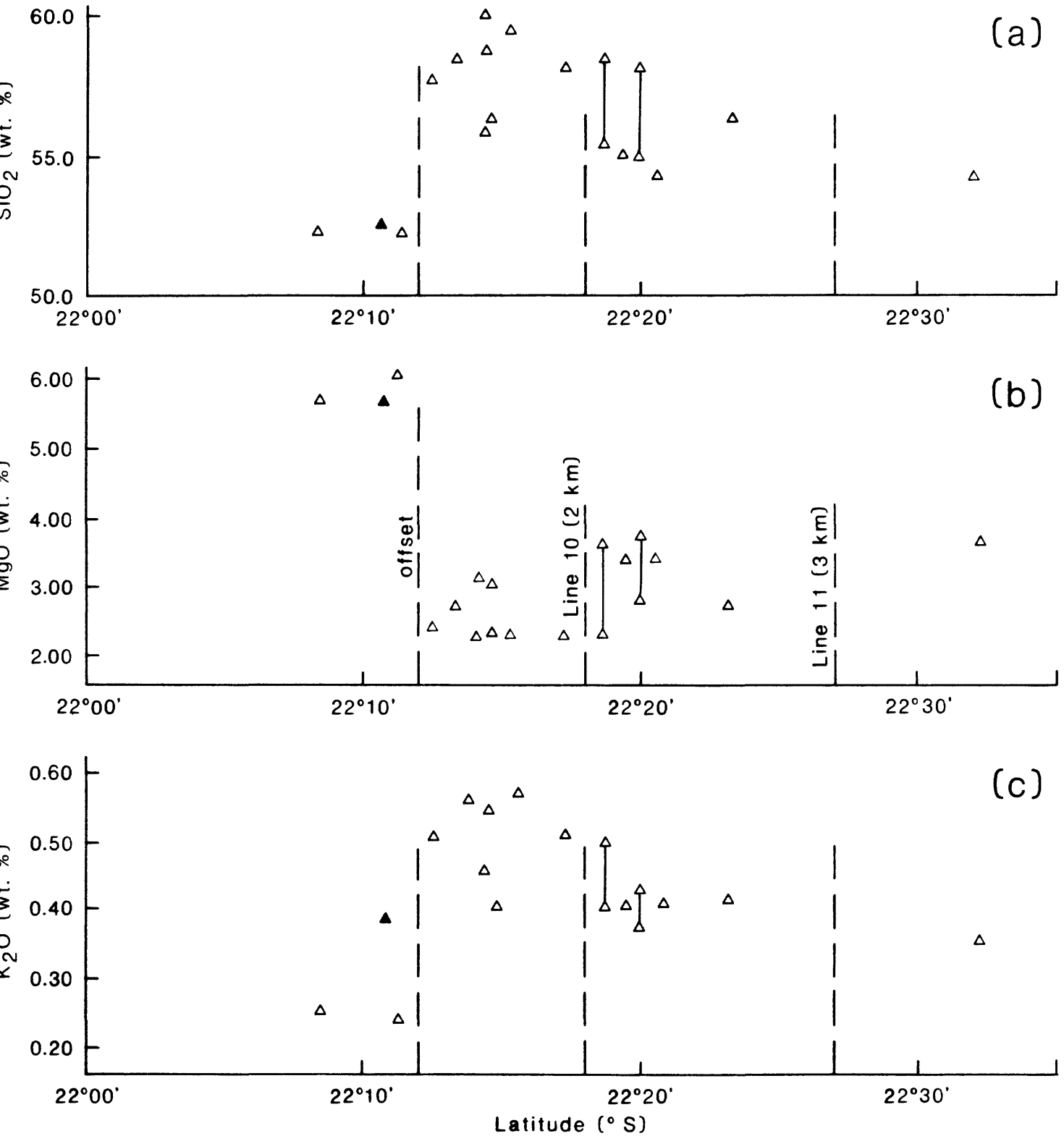
(a)
60.0
55.0
50.0
SiO_2 (wt. %)
22°00'
22°10'
22°20'
22°30'
(b)
6.00
5.00
4.00
3.00
2.00
MgO (wt. %)
offset
Line 10 (2 km)
Line 11 (3 km)
22°00'
22°10'
22°20'
22°30'
(c)
0.60
0.50
0.40
0.30
0.20
K_2O (wt. %)
22°00'
22°10'
22°20'
22°30'
Latitude (° S)

Figure 10